Hypermethylation downregulates P2X$_7$ receptor expression in astrocytoma

JING LIU[1,2], NINGNING LI[1], RUOFAN SHENG[1], RUI WANG[1],
ZUDE XU[1], YING MAO[3], YIN WANG[4] and YING LIU[1]

[1]Department of Pathology, School of Basic Medical Science, Fudan University, Shanghai 200032; [2]Xiawafang Street Community Health Center, Tianjin, Hebei 300220; [3]Department of Neurosurgery, Huashan Hospital; [4]Department of Neuropathology, Institute of Neurology of Huashan Hospital, Fudan University, Shanghai 200040, P.R. China

Abstract. The present study investigated the altered expression of p2X purinoceptor (P2X$_7$R) in astrocytoma. Reverse transcription-quantitative polymerase chain reaction and western blot analysis were used to determine the P2X$_7$R expression in glioblastoma (GBM) and surrounding normal brain tissue. DNA methylation levels of P2X$_7$R gene promoter in GBM were analyzed using a Sequenom MassARRAY® System. Immunohistochemistry (IHC) was used to detect the expression of P2X$_7$R in astrocytoma at different malignancy grades, including diffuse astrocytoma, anaplastic astrocytoma and GBM. P2X$_7$R mRNA and protein were significantly decreased in GBM compared with normal brain tissues. IHC results showed a negative correlation between P2X$_7$R expression and tumor grade. The decreased P2X$_7$R expression was mostly attributed to hypermethylation of its promoter. Therefore, P2X$_7$R was found to perform an important role in tumorigenesis and progression of astrocytoma.

Introduction

Astrocytoma is the most common primary tumor of the central nervous system. The tumor malignancy has been classified according to the histopathological and clinical criteria established by the World Health Organization (WHO). WHO grade IV astrocytoma (glioblastoma; GBM), which is the most invasive form, has a poor prognosis (1). The median survival time of patients with GBM following standard radiation and chemotherapy is 15 months (2)

Under physiological conditions, ATP co-exists with the classical neurotransmitters in vacuoles of synapses, and is released into the extracellular space during signal transmission (3). Exonucleases rapidly degrade extracellular ATP to maintain low physiological concentrations (nM level) (4). However, in a variety of pathological conditions, particularly in tumors, tissue damage accompanied with invasive growth or following surgical removal, chemotherapy and radiotherapy, causes ATP to be released in large quantities from the damaged membranes or directly via toxic transportation (5). The rapid increase in the levels of extracellular ATP (mM level) (5) and activation of purinergic receptors on cell membrane (6) trigger a variety of biological effects.

p2X purinoceptor (P2X$_7$R), activated by high extracellular ATP concentrations, is an ion channel purinergic receptor (7). It is activated into a trimer and forms a membrane pore measuring 4 μm in diameter to allow the passage of 400-900 D ions, including Ca^{2+}, K$^+$ and Na$^+$ (8). The inflow of a large number of basic ions, particularly Ca^{2+}, leads to mitochondrial damage (9), and activates caspases 9, 7 and 3, which mediate cellular apoptosis (10-12). P2X$_7$R-mediated apoptosis controls cell growth under physiological conditions. P2X$_7$R expression in tumors has attracted considerable attention for its unique biological features, since defective apoptosis serves an important role in the development of cancers. In the present study, the expression of P2X$_7$R in astrocytoma was determined to elucidate the mechanisms underlying tumorigenesis and development of astrocytoma.

Materials and methods

Tumor specimens. Human astrocytoma samples were obtained from the Department of Neuropathology, Huashan Hospital, Fudan University (Shanghai, China) for use in this retrospective study. Paraffin-embedded tumor samples (from 100 individuals) included diffuse astrocytomas (grade II; 26 cases), anaplastic astrocytomas (grade III; 28 cases) and GBMs (grade IV; 46 cases). The median age ± standard deviation of the patients was 42.67±17.33 (range, 43-79) years, with a male to female ratio of 3:2 (male, 60 cases; female, 40 cases). Fresh tissues included 7 cases of GBM tumors and the surrounding peripheral brain tissue. All the samples were acquired from individuals who had not received chemotherapy or radiotherapy prior to surgical resection. The procedures

associated with the acquisition of samples from human subjects were approved by the Ethics Committee of Fudan University.

Reverse transcription-quantitative polymerase chain reaction (RT-qPCR). Total RNA from glioma samples were extracted using the QIAamp® RNA Mini kit (Qiagen China Co., Ltd., Shanghai, China) according to the manufacturer's protocol. For the reverse transcription reaction, Takara PrimeScript™ RT Master mix (cat. no. RR036A; Takara Biotechnology Co., Ltd., Dalian, China) was used according to the manufacturer's protocol. qPCR was then performed using SYBR Premix Ex Taq™ (Takara Biotechnology Co., Ltd.) according to the manufacturer's protocol. Equal amounts of each cDNA (100 ng) were amplified in at least 35 cycles of 30 sec at 95˚C, 30 sec at 58˚C, and 1 min at 72˚C. Subsequent to qPCR, a melting curve analysis was performed by gradually increasing the temperature to 95˚C. Data acquisition was performed during the elongation step. The following primers were used: *P2X$_7$R* forward, 5'-TTTAAGCTTATGCCGGCCTGCTGC-AGCTG-3' and reverse, 5'-TTTTTGCGGCCGCTCAGTAAGGACTCT-TGA AGCC-3'; GAPDH forward, 5'-GCACCGTCAAGGCTG AGAAC-3' and reverse, 5'-TGGTGAAGACGCCAGTGGA-3'. GAPDH was used as an endogenous control. Relative quantification was calculated using the $2^{-\Delta\Delta Cq}$ method (13). There were ≥3 replicates performed of each qPCR.

DNA methylation of human glioma samples. Genomic DNA was isolated from fresh tissue using the QIAamp DNA Mini kit (Qiagen China Co., Ltd.) according to the manufacturer's protocol. Bisulfite treatment of genomic DNA was performed using the EpiTect Bisulfite kit (Qiagen China Co., Ltd.) according to the manufacturer's protocol. The cytosine-phosphodiester-guanosine (CpG) island located in the +26/+573 nt region of P2X$_7$R was determined using the Sequenom MassARRAY® system (Sequenom, San Diego, CA, USA) using the following primers: Forward, 5'-AGGAAGAGAGTA TTTTTGTGTAGGTATTTGGGGG-3' and reverse, 5'-CAGT AATACGACTCACTATAGGGAGAAGGCTACATAATAA CAACCTCCCTCCCTAC-3'. The PCR products were directly sequenced using an ABI BigDye Terminator Cycle Sequencing kit (PE Applied Biosystems; Thermo Fisher Scientific, Inc., Waltham, MA, USA) on an ABI 3730 DNA sequencer (Applied Biosystems; Thermo Fisher Scientific, Inc.) according to the manufacturer's protocol. At the corresponding CpG site, the sequencing trace was read as fully or partially methylated (C) and unmethylated (q). Quantitative analysis of CpG methylation was performed using MassCLEAVE base-specific cleavage combined with matrix-assisted laser-desorption ionization-time-of-flight mass spectrometry using EpiTyper software version 4.0 (Sequenom).

Western blot analysis. Tissues were lysed on ice in radioimmunoprecipitation assay buffer (Tris 50 mM, NaCl 0.15 nM, EDTA 10 mM pH 7.4, β-mercaptoethanol 0.1%, Tween-20 0.1% and anti-protease cocktail 1:100) with protease inhibitors and quantified using the bicinchoninic acid method. Protein lysates (50 μg) were resolved using 10% SDS-PAGE and electrotransferred to polyvinylidene fluoride membranes (EMD Millipore, Billerica, MA, USA). Membranes were blocked for 3 h at room temperature with 5% skimmed milk in Tris-buffered saline

with Tween-20 prior to immunoblotting overnight at 4˚C with anti-P2X$_7$R (cat. no. ab93354, Abcam, Cambridge, UK; dilution, 1:300) or anti-β actin (clone AC-40; dilution, 1:50,000; Sigma-Aldrich; Merck KGaA), followed by treatment with the respective secondary antibodies 1 h at room temperature, including horseradish peroxidase (HRP)-conjugated horse anti-mouse IgG (cat. no. PI200) and HRP-conjugated goat anti-rabbit IgG (cat. no. PI1000; dilution, 1:1,000; both Vector Laboratories, Inc., Burlingame, CA, USA). Signals were detected using an enhanced chemiluminescence reaction (ProteinSimple; Bio-Techne, Minneapolis, MN, USA). The intensity of bands was quantified using Gel-Pro Image Analysis software version 32 (Media Cybernetics, Inc., Rockville, MD, USA).

Immunohistochemical analysis. Formalin-fixed, paraffin embedded astrocytoma sections (thickness, 4 μm) were used for immunohistochemistry (IHC) staining using the labeled streptavidin-biotin method (Dako; Agilent Technologies, Inc., Santa Clara, CA, USA). Endogenous peroxidase activity was blocked in deparaffinized slides by incubating sections in 3% H$_2$O$_2$ methanol solution at room temperature for 10 min. Then antigen retrieval was performed with 10 mM citrate buffer (pH 6.0) at 95-100˚C for 10 min. The slides were blocked with 10% goat serum (Abcam) in phosphate-buffered saline for 20 min at room temperature. Primary antibodies included the previously described anti-P2X$_7$R (dilution, 1:200), p53 (cat. no. P9249; dilution, 1:500; Sigma-Aldrich; Merck KGaA), epidermal growth factor receptor (EGFR; cat. no. PB0039; Shanghai Changdao Biotech Co., Ltd., Shanghai, China; dilution, 1:200) and MIB-1 (marker of proliferation, Ki-67; cat. no. sc-101861; dilution, 1:1,000; Santa Cruz Biotechnology, Inc., Dallas, TX, USA). Sections were developed with the rabbit/mouse peroxidase/3,3'-diaminobenzidine EnVision™ Detection kit (cat. no. GK500705; Dako; Agilent Technologies, Inc.) containing the secondary antibody and 3,3'-diaminobenzidine according to the manufacture's protocol, and the nuclei were counterstained with eosin.

The P2X7R and EGFR immunoreactivity scores (IRS) were measured. The fraction (intensity percent; IP) of stained cells was estimated and scored as follows: 0, 0-1%; 1, 2-10%; 2, 11-30%; 3, 31-60%; and 4, 61-100%. The staining intensity (SI) was scored as follows: 0, no staining; 1, weak but definite; 2, moderate; and 3, intense. The IRS was then calculated using the formula: IRS=IP x SI.

The percentages of MIB-1 are presented as the proliferation index (PI). The PI of tumor tissues was expressed as follows: PI% = A x 100/(A + C), where A is the number of MIB-positive cells, and C is the number of counterstained unlabeled cells.

Statistical analysis. Statistical analysis was performed using SPSS 17.0 statistical package (SPSS, Inc., Chicago, IL, USA). Statistical methods included unpaired t-test or one-way analysis of variance, followed by Scheffe's test. Linear correlation analysis was used to examine the association between P2X$_7$R and other parameters of glioma. $P < 0.05$ was considered to indicate a statistically significant difference. Data are expressed as the mean ± standard error of mean.
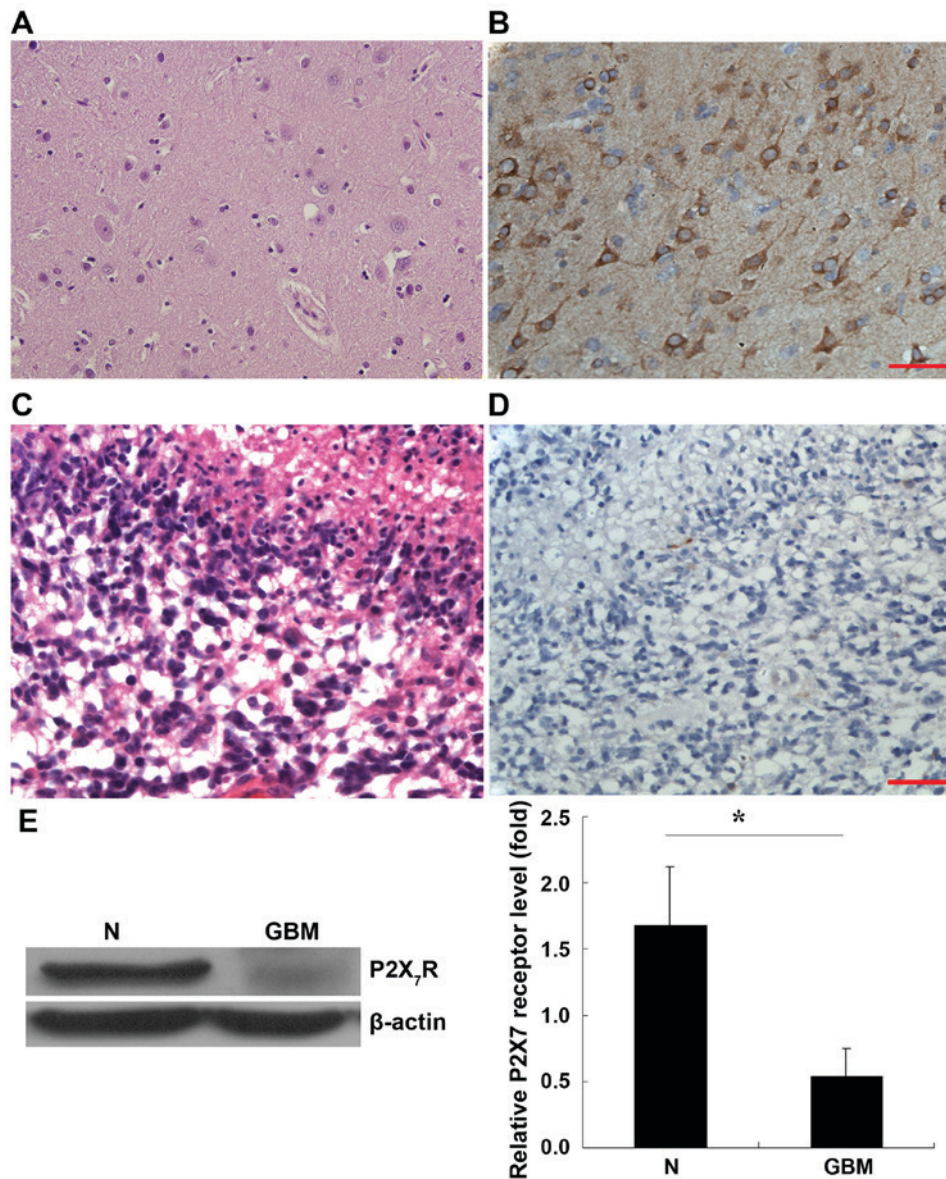
Figure 1. Expression of P2X$_7$R in GBM and normal brain tissue. P2X$_7$R expression was determined by immunohistochemistry staining. (A) H&E staining of normal brain tissue. (B) Normal brain tissue stained for P2X$_7$R expression. (C) H&E staining of GBM. (D) GBM stained for anti-P2X$_7$R expression. (E) Western blot analysis. P2X$_7$R protein was significantly reduced in human GBM compared with the peripheral normal brain tissue. Data are expressed as the mean ± standard error of mean. *P<0.05. Scale bar, 50 μm. P2X$_7$R, p2X purinoceptor; GBM, glioblastoma; H&E, hematoxylin and eosin.

Results

P2X$_7$R expression is significantly lower in astrocytoma compared with the surrounding normal brain tissue. The role of P2X$_7$R in astrocytoma was determined by histologically and immunohistochemically analyzing its expression in normal brain tissue, and astrocytoma. Histological staining of normal brain tissue is presented in Fig. 1A. IHC staining with anti-P2X$_7$R antibody revealed that the cells were positive for P2X$_7$R in the normal brain tissue (Fig. 1B) whereby P2X$_7$R was expressed in the cytoplasm and membrane of these cells. Histological staining of GBM is presented in Fig. 1C. However, IHC revealed that P2X$_7$R expression was almost negative in the tumor (Fig. 1D).

To confirm the expression of P2X$_7$R in these tissues, western blot analysis was performed. As presented in Fig. 1E, normal brain tissue and astrocytoma expressed b-actin at

similar levels, whereas the expression of P2X$_7$R was diminished in GBM samples when compared with peripheral brain tissue. Statistical analysis using 7 paired GBM tissues and their corresponding samples of normal peripheral brain tissue revealed that P2X$_7$R expression was decreased significantly in the GBM (Fig 1E; P<0.05).

Hypermethylation of P2X$_7$R promoter in GBM. P2X$_7$R mRNA was determined using RT-qPCR in the 7 fresh GBM and peripheral brain tissue samples. Consistent with the P2X$_7$R protein expression, the P2X$_7$R mRNA level in GBM was significantly lower compared with that of the peripheral brain tissue (Fig. 2A).

To elucidate the molecular mechanism of the decrease, a DNA methylation assay was performed. As presented in Fig. 2B, a significantly higher level of methylation (mean=0.67±0.1) was observed in GBMs compared with
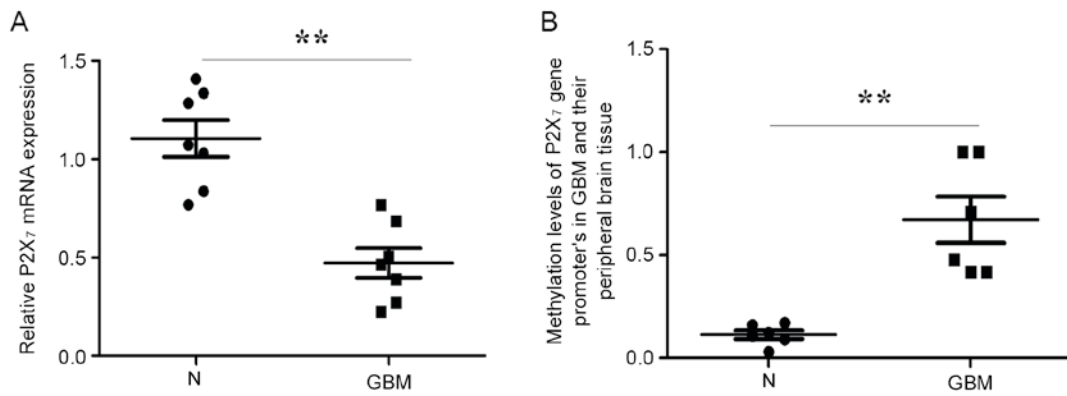
Figure 2. The CpG islands in the +26/+573 nt region of *P2X₇R* were tested with Sequenom MassARRAY® System. (A) In GBM, P2X₇R mRNA levels were lower than in the peripheral brain tissue. (B) P2X₇R gene promoter was hypermethylated compared with the normal brain tissue. An independent-sample t-test was used. Data are expressed as the mean ± standard error of mean. **P<0.01. P2X₇R, p2X purinoceptor; GBM, glioblastoma; N, normal brain tissue.

the surrounding normal brain samples (mean=0.12±0.09) (P=0.046) in the 547-bp region (+26/+573 nt) of the P2X₇R promoter, containing 18 CpG sites. Thus, decreased *P2X₇R* expression in astrocytoma may be associated with hypermethylation of its promoter.

Expression of P2X₇R is negatively associated with malignancy grade in astrocytoma. The expression of P2X₇R in different grades of astrocytoma was then examined. Histological grades of astrocytoma were determined according to nuclear atypia, mitosis, endothelial proliferation and necrosis (Fig. 3). The malignancy level increased from WHO grade II to IV. As presented in Fig. 3A, C and E, histological staining revealed a marked increase in cell density, nuclear heteromorphism, and caryokinesis between grade II and IV. By contrast, IHC staining revealed that the expression of P2X₇R decreased correspondingly (Fig. 3B, D and F). Thus, the expression of P2X₇R may be negatively associated with the malignancy of astrocytoma (Fig. 3G).

In addition, it was confirmed that P2X₇R was negatively correlated with the proliferation index of MIB-1 (r=-0.411; P<0.01). No correlation was identified between P2X₇R, and cumulative p53 or EGFR expression in the astrocytoma (data not shown).

Discussion

P2X₇R-mediated apoptosis depends on P2X₇R expression (14). The expression of P2X₇R did not differ significantly between normal colon epithelial cells and colon cancer cells (15). However, thyroid cancer cells exhibit higher P2X₇R expression compared with the normal cells (16). The P2X₇R expression has be revealed to be decreased in early phases of neoplasia of the ectoderm (skin and breast) (17,18), the distal paramesonephric duct (endocervix and endometrium) (19), and the urogenital sinus (bladder and ectocervix) (20,21). However, the expression of P2X₇R in brain tumor remains elusive.

Diffuse infiltration of glioma is a major therapeutic challenge for definitive surgical resection. It limits the efficacy of other local therapies, leading to local recurrence and short survival. In GBM, areas, including the tumor center distal to the capillaries often become hypoxic and undergo necrosis.

Such regions are considered to contain higher concentrations of extracellular ATP (22). Activation of P2X₇R in glioma C6 cells leads to increased mobilization of intracellular calcium, formation of large pores and enhanced expression of several pro-inflammatory factors (23). The tumor suppressor role of P2X₇R has been attributed to its pro-inflammatory and pro-apoptotic function (24). Consistent with this hypothesis, activation of P2X₇R in astrocytes leads to a state of reversible growth arrest (25). These data were obtained from mouse GBM or normal astrocyte cells. Using fresh human GBM and surrounding brain tissue samples, the present study revealed that the expression of P2X₇R mRNA, and protein was significantly decreased. However, another immunohistochemical study reported the elevated expression of P2X₇R in glioma (24). In the present study, using 100 astrocytoma samples at different malignant grades, P2X₇R expression was identified to be negatively correlated with the malignancy of astrocytoma.

Generally, methylation at CpG islands in a gene promoter favors transcriptional repression (25). DNA cytosine methylation is one of the most consistent epigenetic alterations in various types of human cancer (26). DNA hypermethylation is an essential epigenetic mechanism for the silencing of numerous genes, including those involving cell cycle regulation, receptors, DNA repair and apoptosis. The present study revealed that P2X₇R genes were hypermethylated at the CpG sites in the +26/+573 nt region of human astrocytoma samples. These results indicate that the decrease in P2X₇R expression may be associated with hypermethylation of its gene promoter.

Previous studies have demonstrated that P2X₇R exhibits significant growth-promoting effects *in vivo* (27,28), inducing extensive neovascularization and elevated levels of VEGF, and thereby promoting cell invasion and migration (29). However, the exact molecular basis of P2X₇R-mediated growth-promoting activity is unclear. By contrast, P2X₇R suppression induced the growth of glioma by directly promoting cell proliferation and angiogenesis (30). Functional P2X₇R activation by ATP resulted in rapid cytotoxicity affecting cell growth and survival, leading to inhibition of tumor growth *in vitro,* and *in vivo* (31,32). P2X₇R expression was also identified to be negatively correlated with a high proliferation index of glioma in the present study. Therefore,
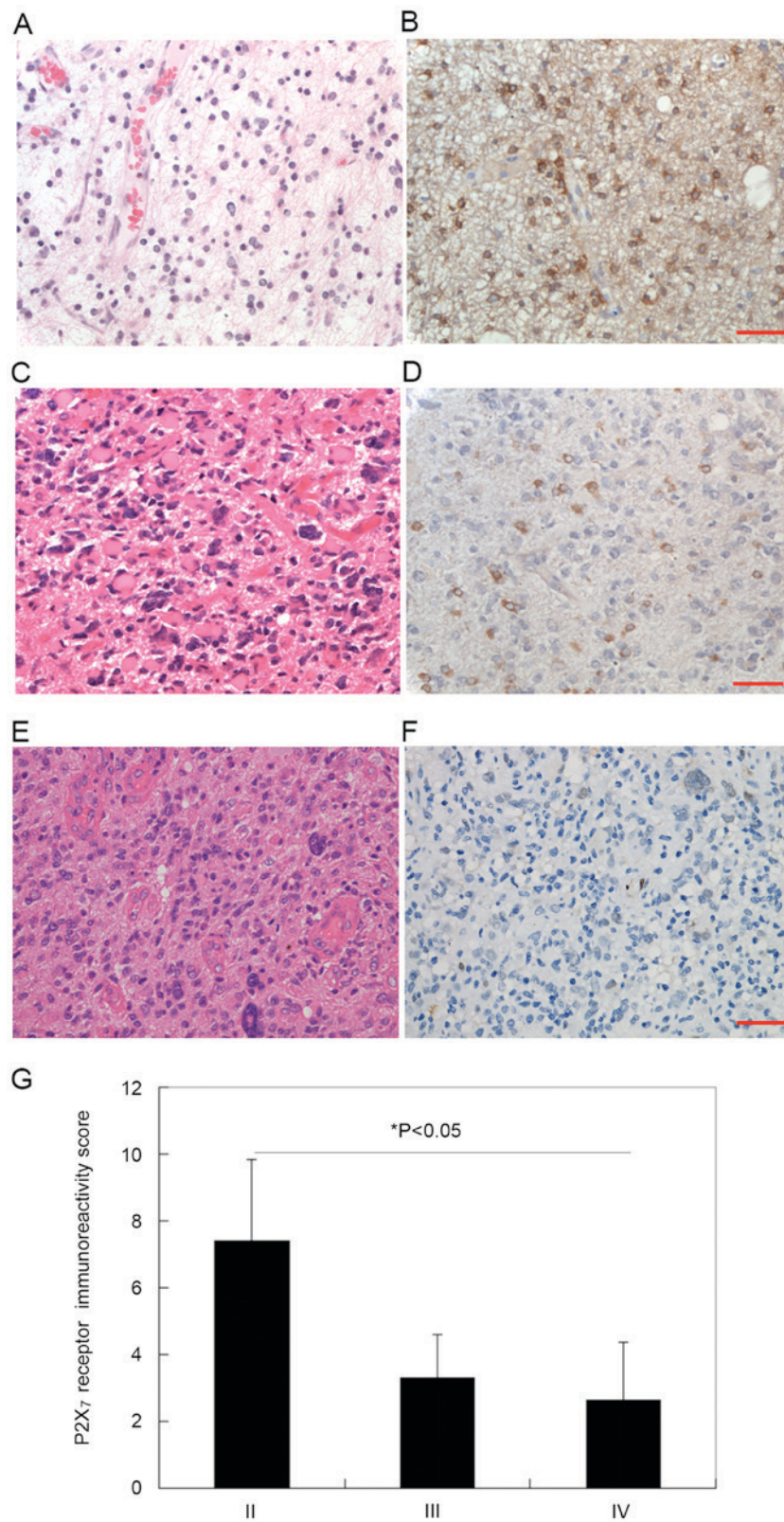
Figure 3. IHC staining with an anti-P2X$_7$R antibody in human astroglioma grades II to IV. (A) Representative grade II diffuse astrocytoma. (B) Representative grade II anaplastic astrocytoma with P2X$_7$R staining. (C) Representative grade III anaplastic astrocytoma. (D) Representative grade III diffuse astrocytoma with P2X$_7$R staining. (E) Representative grade IV glioblastoma. (F) Representative grade IV glioblastoma with P2X$_7$R staining. (G) Graph of the IHC scores for P2X$_7$R in glioma samples. The P2X$_7$R expression was negatively correlated with the malignancy of astrocytoma. A one-way analysis of variance followed by Scheffe's test was used for multiple comparisons. Data are presented as the mean ± standard error of mean. *$P<0.05$. Scale bar, 50 μm. IHC, immunohistochemistry; P2X$_7$R, p2X purinoceptor.

the decrease in P2X$_7$R expression may have an important role in the development and progression of astrocytoma.

In the present study, compared with the tumor tissue, the surrounding normal brain tissue demonstrated high P2X$_7$R

immunoreactivity. Thus, we hypothesize that the normal brain cells may become apoptotic following P2X$_7$R activation, thus accommodating tumor cells. As a consequence, P2X$_7$R expression in normal brain cells enhances the infiltration and proliferation of the glioma. Contrary to this, a higher P2X$_7$R expression in astroglioma may increase the response to radiotherapy (33). Therefore, increasing the malignancy and decreasing P2X$_7$R expression of astroglioma may lead to higher therapeutic resistance.

In conclusion, the results indicated that the levels of P2X$_7$R were lower in astrocytoma tissues compared with the normal surrounding brain tissue. Inhibition of the P2X$_7$R-mediated apoptosis in the peripheral normal brain tissue surrounding the tumor may limit glioma infiltration and growth. Therefore, it is important to understand P2X$_7$R expression and its function in glioma, and normal brain cells to develop appropriate chemotherapeutic interventions *in vivo*.

Acknowledgements

References

1. Cavenee W K, Leung S, Hawkins C, *et al*: WHO Classification of Tumours of the Central Nervous System, Revised. Fourth Edition, WHO Press, Geneva, Switzerland, pp28-45, 2016.
2. Johnson DR and O'Neill BP: Glioblastoma survival in the United States before and during the temozolomide era. J Neurooncol 107: 359-364, 2012.
3. Cotrina ML, Lin JH, López-García JC, Naus CC and Nedergaard M: ATP-mediated glia signaling. J Neurosci 20: 2835-2844, 2000.
4. Zimmermann H: Extracellular metabolism of ATP and other nucleotides. Naunyn Schmiedebergs Arch Pharmacol 362: 299-309, 2003.
5. Ciccarelli R, Ballerini P, Sabatino G, Rathbone MP, D'Onofrio M, Caciagli F and Di Lorio P: Involvement of astrocytes in purine-mediated reparative processes in the brain. Int J Dev Neurosci 19: 395-414, 2001.
6. Ralevic V and Burnstock G: Receptors for purines and pyrimidines. Pharmacol Rev 50: 413-492, 1998.
7. Di Virgilio F: Dr. Jekyll/Mr. Hyde: The dual role of extracellular ATP. J Auton Nerv Syst 81: 59-63, 2000.
8. Kim M, Jiang LH, Wilson HL, North RA and Surprenant A: Proteomic and functional evidence for a P2X7 receptor signalling complex. EMBO J 20: 6347-6358, 2001.
9. Wang L, Feng YH and Gorodeski GI: Epidermal growth factor facilitates epinephrine inhibition of P2X7-receptor-mediated pore formation and apoptosis: A novel signaling network. Endocrinology 146: 164-174, 2005.
10. Schneider EM, Vorlaender K, Ma X, Du W and Weiss M: Role of ATP in trauma-associated cytokine release and apoptosis by P2X7 ion channel stimulation. Ann NY Acad Sci 1090: 245-252, 2006.
11. Bulanova E, Budagian V, Orinska Z, Hein M, Petersen F, Thon L, Adam D and Bulfone-Paus S: Extracellular ATP induces cytokine expression and apoptosis through P2X7 receptor in murine mast cells. J Immunol 174: 3880-3890, 2005.
12. Said T, Dutot M, Christon R, Beaudeux JL, Martin C, Warnet JM and Rat P: Benefits and side effects of different vegetable oil vectors on apoptosis, oxidative stress, and P2X7 cell death receptor activation. Invest Ophthalmol Vis Sci 48: 5000-5006, 2007.
13. Livak KJ and Schmittgen TD: Analysis of relative gene expression data using real-time quantitative PCR and the 2(-Delta Delta C(T)) method. Methods 25: 402-408, 2001.
14. Feng YH, Wang L, Wang Q, Li X, Zeng R and Gorodeski GI: ATP stimulates GRK-3 phosphorylation and beta-arrestin-2-dependent internalization of P2X7 receptor. Am J Physiol Cell Physiol 288: C1342-C1356, 2005.
15. Li X, Qi X, Zhou L, Fu W, Abdul-Karim FW, Maclennan G and Gorodeski GI: P2X(7) receptor expression is decreased in epithelial cancer cells of ectodermal, uro-genital sinus and distal paramesonephric duct origin. Purinergic Signal 5: 351-368, 2009.
16. Solini A, Cuccato S, Ferrari D, Santini E, Gulinelli S, Callegari MG, Dardano A, Faviana P, Madec S, Di Virgilio F and Monzani F: Increased P2X7 receptor expression and function in thyroid papillary cancer: A new potential marker of the disease? Endocrinology 149: 389-396, 2008.
17. Fu W, McCormick T, Qi X, Luo L, Zhou L, Li X, Wang BC, Gibbons HE, Abdul-Karim FW and Gorodeski GI: Activation of P2X(7)-mediated apoptosis Inhibits DMBA/TPA-induced formation of skin papillomas and cancer in mice. BMC Cancer 9: 114, 2009.
18. Greig AV, Linge C, Healy V, Lim P, Clayton E, Rustin MH, McGrouther DA and Burnstock G: Expression of purinergic receptors in non-melanoma skin cancers and their functional roles in A431 cells. J Invest Dermatol 121: 315-327, 2003.
19. Li X, Qi X, Zhou L, Catera D, Rote NS, Potashkin J, Abdul-Karim FW and Gorodeski GI: Decreased expression of P2X7 in endometrial epithelial pre-cancerous and cancer cells. Gynecol Oncol 106: 233-243, 2007.
20. Lee HY, Bardini M and Burnstock G: Distribution of P2X receptors in the urinary bladder and the ureter of the rat. J Urol 163: 2002-2007, 2000.
21. Li X, Zhou L, Feng YH, Abdul-Karim FW and Gorodeski GI: The P2X7 receptor: A novel biomarker of uterine epithelial cancers. Cancer Epidemiol Biomarkers Prev 15: 1906-1913, 2006.
22. Wei W, Ryu JK, Choi HB and McLarnon JG: Expression and function of the P2X(7) receptor in rat C6 glioma cells. Cancer Lett 260: 79-87, 2008.
23. Fang KM, Wang YL, Huang MC, Sun SH, Cheng H and Tzeng SF: Expression of macrophage inflammatory protein-1α and monocyte chemoattractant protein-1 in glioma-infiltrating microglia: Involvement of ATP and P2X7 receptor. J Neurosci Res 89: 199-211, 2011.
24. Ryu JK, Jantaratnotai N, Serrano-Perez MC, McGeer PL and McLarnon JG: Block of purinergic P2X7R inhibits tumor growth in a C6 glioma brain tumor animal model. J Neuropathol Exp Neurol 70: 13-22, 2011.
25. Zilberman D and Henikoff S: Genome-wide analysis of DNA methylation patterns. Development 134: 3959-3965, 2007.
26. Esteller M: CpG island hypermethylation and tumor suppressor genes: A booming present, a brighter future. Oncogene 21: 5427-5440, 2002.
27. Gómez-Villafuertes R, García-Huerta P, Díaz-Hernández JI and Miras-Portugal MT: PI3K/Akt signaling pathway triggers P2X7 receptor expression as a pro-survival factor of neuroblastoma cells under limiting growth conditions. Sci Rep 5: 18417, 2015.
28. Braganhol E, Kukulski F, Lévesque SA, Fausther M, Lavoie EG, Zanotto-Filho A, Bergamin LS, Pelletier J, Bahrami F, Ben Yebdri F, *et al*: Nucleotide receptors control IL-8/CXCL8 and MCP-1/CCL2 secretions as well as proliferation in human glioma cells. Biochim Biophys Acta 1852: 120-130, 2015.
29. Qiu Y, Li WH, Zhang HQ, Liu Y, Tian XX and Fang WG: P2X7 mediates ATP-driven invasiveness in prostate cancer cells. PLoS One 9: e114371, 2014.
30. Fang J, Chen X, Zhang L, Chen J, Liang Y, Li X, Xiang J, Wang L, Guo G, Zhang B and Zhang W: P2X7R suppression promotes glioma growth through epidermal growth factor receptor signal pathway. Int J Biochem Cell Biol 45: 1109-1120, 2013.
31. White N, Butler PE and Burnstock G: Human melanomas express functional P2X(7) receptors. Cell Tissue Res 321: 411-418, 2005.
32. Bian S, Sun X, Bai A, Zhang C, Li L, Enjyoji K, Junger WG, Robson SC and Wu Y: P2X7 integrates PI3K/AKT and AMPK-PRAS40-mTOR signaling pathways to mediate tumor cell death. PLoS One 8: e60184, 2013.
33. Gehring MP, Kipper F, Nicoletti NF, Sperotto ND, Zanin R, Tamajusuku AS, Flores DG, Meurer L, Roesler R, Filho AB, *et al*: P2X7 receptor as predictor gene for glioma radiosensitivity and median survival. Int J Biochem Cell Biol 68: 92-100, 2015.